Electronic Supplementary Information

An upgraded 2D nanosheet-based FRET biosensor: Insights to avoid background and eliminate effects of background fluctuations†

Suli Jia,[‡a] Chengquan Wang,[‡b] Jing Qian,[*a] Xingcai Zhang,[c,d] Haining Cui,[a] Qi Zhang,[a] Yunmeng Tian,[a] Nan Hao,[a] Jie Wei[a] and Kun Wang[*a]

[a]*School of Chemistry and Chemical Engineering, Jiangsu University, Zhenjiang 212013, PR China*

[b]*School of Food and Biological Engineering, Jiangsu University, Zhenjiang 212013, PR China.*

[c]*John A. Paulson School of Engineering and Applied Sciences, Harvard University, Cambridge, MA, 02138, USA*

[d]*School of Engineering, Massachusetts Institute of Technology, Cambridge, MA, 02139, USA*

‡ Authors contributed equally to this work.

*Corresponding author: E-mail addresses: qianj@ujs.edu.cn (J. Qian); wangkun@ujs.edu.cn (K. Wang)

Materials and reagents. Sodium acetate (CH_3COONa), $FeCl_3 \cdot 6H_2O$, ethylene glycol (EG), diethylene glycol (DEG), polyethylene glycol (PEG), thiourea (CN_2H_4S), $(NH_4)_6Mo_7O_{24} \cdot 4H_2O$, citric acid (CA), urea (CH_4N_2O), NaOH, N-hydroxysuccinimide (NHS), 1-ethyl-3-(3-dimethylaminopropyl) carbodiimide hydrochloride (EDC), AFB1, ochratoxin A (OTA), fumonisin B1 (FB1), zearalenone (ZEN), deoxynivalenol (DON), and tris (hydroxymethyl) aminomethane (Tris) involved in our research were of analytical grade and were purchased from Sinopharm Chemical Reagent Co., Ltd. (China). We obtain the AFB1 aptamer sequence (5'-NH_2-GTT GGG CAC GTG TTG TCT CTC TGT GTC TCG TGC CCT TCG CTA GGC CC-3') from Sangon Biotech Co., Ltd (Shanghai, China). Deionized water was used in all of the experimental procedure. 10 mM Tris-HCl buffer (pH 7.4) was used for biosensor fabrication and detection process.

Apparatus. UV-vis absorption spectra were measured by UV-2450 spectrophotometer (Shimadzu, Japan) at room temperature. Fourier transform infrared (FT-IR) spectra of the samples were carried out by Spectrometer (Nicolet Nexus 470 FT-IR). Fluorescence spectra were obtained from fluorospectro photometer (Hitachi F-4500). The morphology of the samples was checked by transmission electron microscopy (TEM) technique (JEOL 2100, JEOL, Japan) and field emission scanning electron microscope (SEM, JSM-7001F, JEOL, Japan). X-ray photoelectron spectroscopy (XPS) was taken on an ESCALAB 250 multi-technique surface analysis system (Thermo Electron Co., USA). X-ray diffraction (XRD) patterns were obtained using a D8 X-ray diffractometer equipped with (Bruker, Germany) high-intensity Cu Kα (λ = 1.5406 Å) radiation.

Experimental section

Preparation of Fe_3O_4 nanospheres. Firstly, 0.5536 g $FeCl_3 \cdot 6H_2O$ was dissolved in the mixture of 10 mL EG and 10 mL DEG, then adding 1.5 g CH_3COONa and 1.0 g PEG to above mixture, followed by 30 min-stirring. The resultant mixture was transferred into a Teflon-lined stainless-steel autoclave and reacted at 200 °C for 6 h. After naturally cooling down to room temperature, the black precipitate was magnetically collected and washed with water and ethanol for several times and then dried at 60 °C under vacuum overnight.

Synthesis of NGQDs. Firstly, 20 mL CA (40 mg mL^{-1}) and urea (7.2 mg mL^{-1}) evenly mixed and transferred to a 25 mL Teflon-lined stainless-steel autoclave and reacted at 180 °C for 8 h. After cooling to room temperature, the products were transferred to a beaker and adjusted the pH value to 7.0 with NaOH (5 mg mL^{-1}). The mixture was mixed with excessive ethanol and allowed to stand for 15 min, then centrifuged at 13,000 rpm for 5 min to collect NGQDs. The purified NGQDs were re-dispersed in 20 mL water and stored in a brown bottle at 4 °C for later use.

Preparation of Fe_3O_4@MoS_2 hybrids. Preparation of Fe_3O_4@MoS_2 hybrids was achieved by a solvothermal method. First, both 0.76 g of thiourea and 0.35 g of $(NH_4)_6Mo_7O_{24} \cdot 4H_2O$ were dissolved in water (10 mL) and ultrasonically treated to obtain a homogeneous solution. Then, 20 mg of Fe_3O_4 nanospheres was transferred to above solution and ultrasonically treated for 10 min to form the uniform suspension, which was transferred to a 25 mL Teflon-lined stainless-steel autoclave at 200 °C for 10 h. After cooling down to room temperature, the black product was collected by magnetic separation and washed for three times with water and then drying under vacuum at 80 °C for 10 h. For comparison, MoS_2 nanosheets were obtained by a similar procedure (without the introducing of Fe_3O_4 nanospheres) which were collected by centrifugation at 12000 rpm for half an hour.

Preparation of NGQDs labeled report probe. For conjugation of aptamer on NGQDs, a mixture of NGQDs solution (5 mL), EDC solution (100 μL, 200 μM), and NHS solution (100 μL, 200 μM) were oscillated for 2 h to activate these carboxyl groups on NGQDs surface. Subsequently, 20 μL aptamer was added to above mixed solution and stirred for 24 h under room temperature. The resultant NGQDs/aptamer report probes were centrifuged at 10000

rpm for 15 min and washed with Tris-HCl buffer for several times. Finally, the collected NGQDs/aptamer report probes were dispersed in 5 mL Tris-HCl buffer and maintained at 4 °C for subsequent experiments.

Preparation of the FRET-based biosensor. To fabricate the FRET-based biosensor, the as-prepared Fe_3O_4@MoS_2 hybrids were sonicated for 30 min to sufficiently disperse the materials. Firstly, 100 μL of NGQDs/aptamer solution was added to 300 μL Fe_3O_4@MoS_2 suspension (5 mg mL^{-1}), after reacting for 8 min at room temperature, we removed the un-adsorbed NGQDs/aptamer probes by magnetic separation and washed with Tris-HCl buffer for several times to obtain the Fe_3O_4@MoS_2-NGQDs/aptamer bioconjugations and used as the FRET-based biosensor for subsequent detection. The amount of aptamer immobilized on the Fe_3O_4@MoS_2 hybrids (per 1.5 mg) were determined to be 2.2 ng by a One Drop™ OD-1000 spectrophotometer (Thermo Fisher Scientific, Waltham, USA) at 260 nm.

Detection procedure. 100 μL AFB1 solution with different concentrations was added to as-obtained bioconjugations (Fe_3O_4@MoS_2-NGQDs/aptamer), and incubated at 37 °C for 40 min, which was diluted with Tris-HCl buffer to reach a final volume of 700 μL, then quickly obtained the supernatant using hand-held 30 s magnetic separation and performed fluorescence detection.

Preparation of peanut samples. Firstly, 11 g of peanut samples was grinded together with 1 g of sodium chloride, and then divided equally into 3 portions of 4 g each. After that, 10 mL of the extraction solution (methanol: water=6:4 (v/v)) was introduced, and then centrifuged by centrifugation at 6000 rpm for 10 min to remove the precipitate. All samples were analyzed for AFB1 content using HPLC to ensure that they were free from AFB1 before used. Subsequently, the peanut sample was passed through a 0.45 mm syringe filter. Finally, equal volumes of different concentrations of AFB1 (0.1 ng mL^{-1}, 1 ng mL^{-1}, and 5 ng mL^{-1}) standards were added to aliquots of sample mixture and mixed thoroughly by shaken for 30 min, the pH was adjusted to 7.4 for later use.

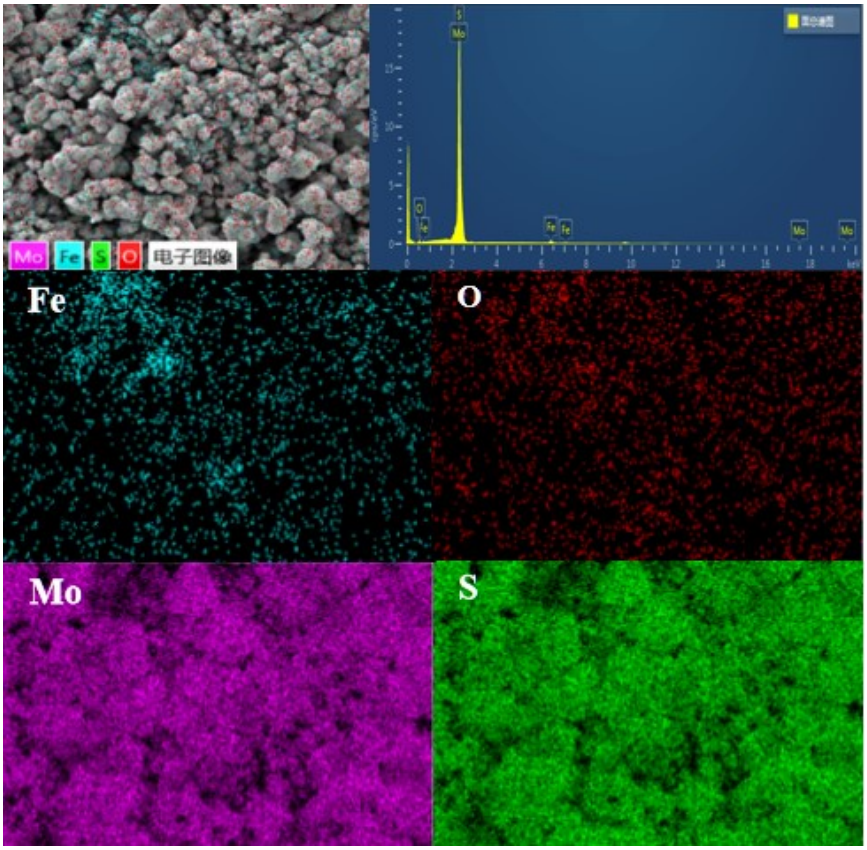

Fig. S1 EDS analysis and the corresponding elements mapping of MoS_2@Fe_3O_4 hybrids.

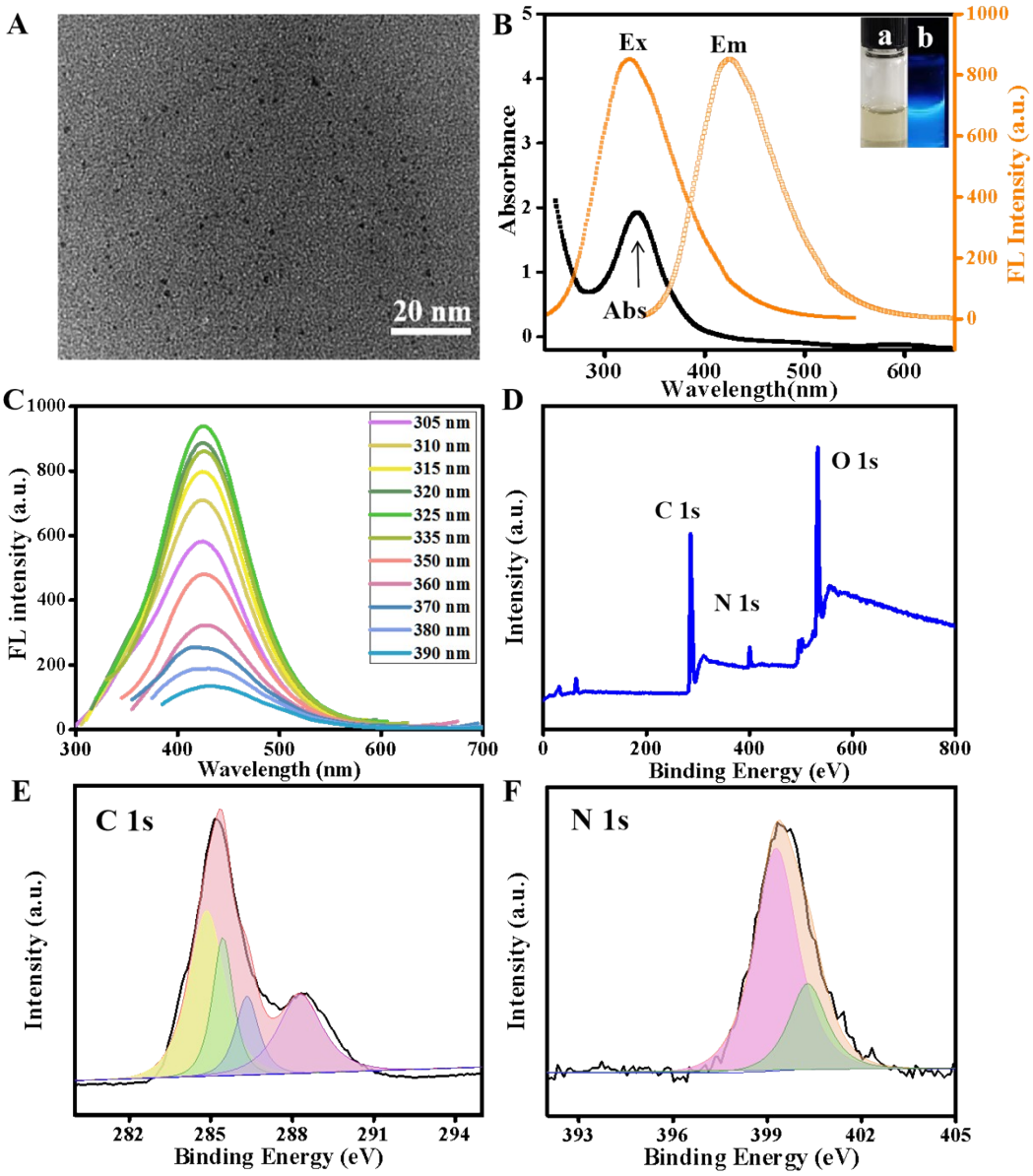

Fig. S2 (A) TEM image of NGQDs (B) UV-vis absorption spectrum and the fluorescence excitation (Ex) and emission (Em) spectra of the as-prepared NGQDs in aqueous solution. Inset: Photographs of NGQDs solution taken under (a) visible-light and (b) 365 nm UV light. (C) FL spectra of the NGQDs at various excitation wavelengths (from 305 to 390 nm). XPS spectra of the as-prepared NGQDs: (D) survey spectra, (E) C 1s, and (F) N 1s.

Characterization of the resultant NGQDs. From Fig. S2A we can notice the particle size of the resultant NGQDs was relatively uniform (around 3 nm) and evenly dispersed. Its well-defined absorption peak position of NGQDs was appeared at 338 nm while the fluorescence spectroscopy indicated that the optimal maximum excitation and emission wavelength was at

325 and 426 nm, respectively (Fig. S2B). Inset of Fig. S2B illustrates that the aqueous dispersion of NGQDs solution displayed light yellow color under visible-light (photograph a) and emitted strong blue fluorescence under 365 nm UV irradiation (photograph b). Under different excitation wavelengths, the position of the emission peak of NGQDs remained unchanged, but the fluorescence intensity changed (Fig. S2C). This indicates that the emission wavelength of NGQDs is independent of the excitation wavelength which resulted from the high crystallinity and high uniformity in size of the resultant NGQDs.[1] When the excitation wavelength was 325 nm, the fluorescence intensity for emission peak was the largest, which was used as the excitation wavelength for detection procedure.

X-ray photoelectron spectroscopy (XPS) measurements were performed to demonstrate the elements structure and valence states of the as-prepared NGQDs. The survey XPS spectrum of NGQDs indicated the sample contained carbon, nitrogen, and oxygen elements (Fig. S2D). Fig. S2E showed the high-resolution C 1s spectrum, the peaks at 284.6, 285.2, 286.1, and 288.2 eV are corresponded to C-C, C-N, C-O and O-C=O bonds, respectively.[2-4] Fig. S2F revealed the narrow scan N 1s XPS spectrum which can deconvolve into two peaks located at 399.2 and 400.5 eV, attributing to pyridine-type N and pyrrolic-type N.[5] All above XPS analysis have proved that N atoms had been successfully doped into GQDs and the as-obtained NGQDs had abundant nitrogen and oxygen-containing groups on their surfaces.[6]

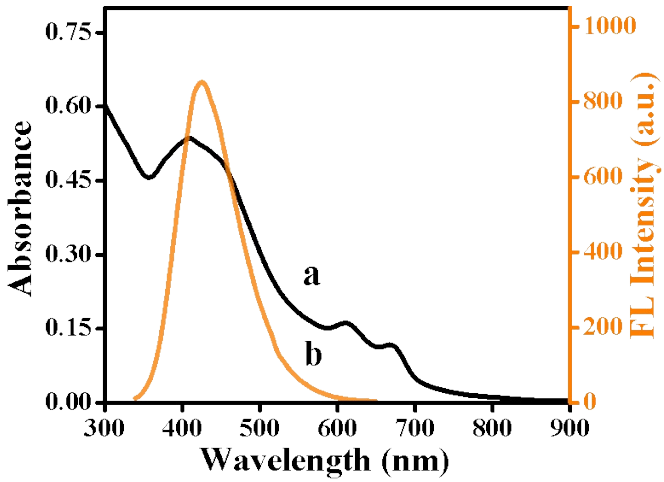

Fig. S3 The spectral overlap between the (a) UV–vis absorption spectrum of MoS_2 nanosheets and (b) fluorescence spectrum of NGQDs.

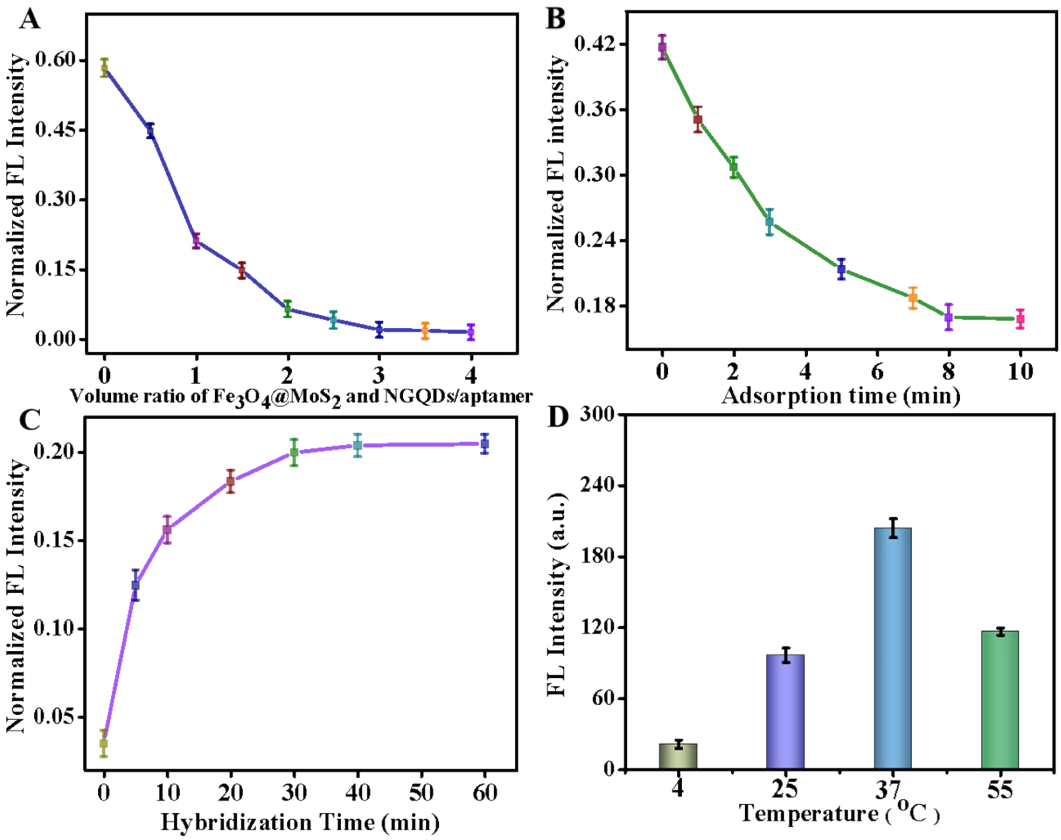

Fig. S4 (A) The fluorescence intensity of difference volume ratio between Fe_3O_4@MoS_2 suspension and NGQDs/aptamer solution. (B) Effect of the reaction time of Fe_3O_4@MoS_2 and NGQDs/aptamer. Effect of the (C) binding time and (D) incubation temperature between biosensor and AFB1 (10 ng mL^{-1}).

Optimization of important parameters. In order to obtain a high-efficiency biosensor, it is critical to optimize some important experimental conditions. Fe_3O_4@MoS_2 hybrids were used as both magneto-controlled substrates and fluorescence quenchers in the detection scheme. Therefore, their amount has an important influence on fluorescence quenching in the reaction system. The effect of the volume ratio between the Fe_3O_4@MoS_2 suspension and the NGQDs/aptamer solution on fluorescence quenching was explored by fixing the volume of NGQDs/aptamer (100 μL) and varying the volume of Fe_3O_4@MoS_2 suspension. To avoid the influence of the volume change on the experiment, the total volume was of test solution were set at 700 μL by adding Tris-HCl buffer before performing the fluorescence detection. As shown in Fig. S4A, upon the increasing volume ratio between Fe_3O_4@MoS_2 suspension and the NGQDs/aptamer solution, the fluorescence intensity for the test solution dropped

dramatically with the volume ratio increasing from 0 to 3:1 and tended to be flat beyond 3:1. As a consequence, 3:1 was selected as the ideal volume ratio to construct the biosensor.

In addition, reaction time between Fe_3O_4@MoS_2 and NGQDs/aptamer also plays a key role in the fluorescence quenching process. Aim to obtain the optimized adsorption time, we mixed 300 μL Fe_3O_4@MoS_2 suspension and 100 μL NGQDs/aptamer solution together, and then the fluorescence intensity of the mixture within 0-10 min was recorded. As indicated from Fig. S4B, the recorded fluorescence intensity decreased while it started to stabilize at 8 min. In order to shorten the entire detection time, we selected 8 min as the optimal reaction time between Fe_3O_4@MoS_2 and NGQDs/aptamer. Furthermore, the incubation time of NGQDs/aptamer and AFB1 is also a time-dependent process. The fluorescence intensity of the released NGQDs/aptamer was measured within a time period of 0-60 min (Fig. S4C). As noted, fluorescence intensity of the released NGQDs/aptamer increased continuously within 0-40 min and did not change after 40 min. On this basis, the optimal incubation time was determined to be 40 min for subsequent detection. Additionally, the influence of the incubation temperature on the binding reaction was also investigated (Fig. S4D). The results revealed that the fluorescence recovery was the strongest when the biosensor incubated at 37 °C, which was selected as the optimal incubation temperature for the binding reaction between aptamer and AFB1.

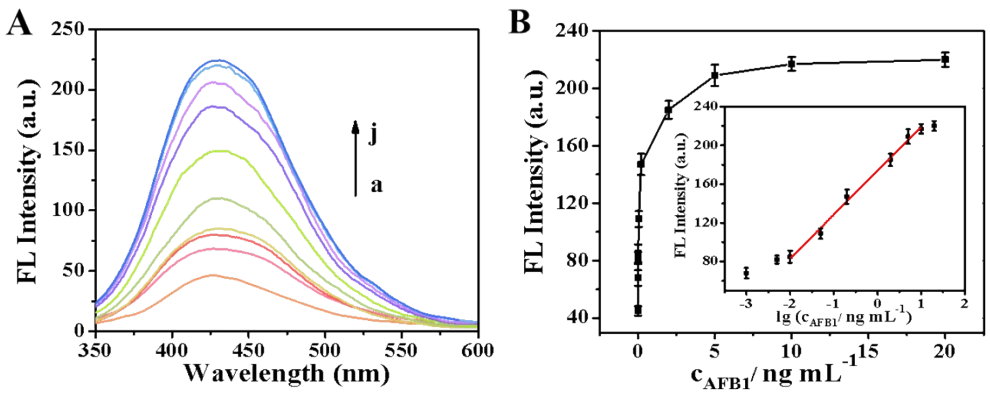

Fig. S5 (A) Fluorescence Intensity of biosensor based on pristine MoS_2 nanosheets and NGQDs/aptamer at different AFB1 concentrations (from a to j: blank, 0.001, 0.005, 0.01, 0.05, 0.2, 2, 5, 10, and 20 ng mL^{-1}). (B) Relationship between AFB1 concentration and fluorescence intensity. Inset shows the calibration curve obtained with the fluorescence intensity versus the logarithm of AFB1 concentration.

Table S1 Comparison of the analytical performance between the FRET and upgraded FRET biosensors for AFB1 detection.

Methods	Recognition Probe	Linear range (ng mL^{-1})	LOD (pg mL^{-1})	Reference
FRET	antibody	0.06-5	40	7
	antibody	1-10	850	8
	aptamer	3.1-124.8	1060	9
	aptamer	0.005-300	2.67	10
	aptamer	0.01-10	3.3	11
Upgraded FRET	aptamer	0.001-10	0.31	This work

The parallel experiments were conducted by incubating the biosensor with AFB1 (1 ng mL^{-1}) for five times. The RSD was calculated to be 4.2%, indicating that this biosensor possessed a satisfied reproducibility. In addition, we investigated the long-term stability by detecting the fluorescence response when the biosensor incubated with 10 ng mL^{-1} AFB1 one month later. The experimental results showed that the biosensor still possessed 92.3% response of the initial response, indicating it had good long-term stability.

Table S2 Results of determination of AFB1 in spiked peanut samples (n = 3).

Sample	Added (pg mL^{-1})	Found (pg mL^{-1}) (mean ± SD)(n=3)	RSD (%)	Recovery (%)
1	0.1	0.101 ±0.007	6.5	101.25
2	1	0.983 ±0.035	7.4	98.36
3	5	5.03 ±0.05	7.8	100.62

To explore the potential and practical application of the proposed biosensor, we measured the recoveries percentage of AFB1 in peanut samples. As shown in Table S2, the peanut samples were spiked with standard AFB1 at 0.1, 1, and 5 ng mL^{-1} for test, with the recoveries range of AFB1 were from 98.36% to 101.25% with RSD < 7.8%. This result demonstrates that the constructed biosensor have potential application in real samples analysis.

Notes and references

1 C. Wang, J. Qian, K. Wang, M. Hua, Q. Liu, N. Hao, T. You and X. Huang, *ACS Appl. Mater. Interfaces*, 2015, **7**, 26865-26873.

2 Y. Yin, Q. Liu, D. Jiang, X. Du, J. Qian, H. Mao and K. Wang, *Carbon*, 2016, **96**, 1157-1165.

3 F. Wang, X. Fu, X. Chai, Q. Han, H. Wang and Q. Hao, *Microchem. J.*, 2021, **168**, 106389.

4 L. Zhang, Z.-Y. Zhang, R.-P. Liang, Y.-H. Li and J.-D. Qiu, *Anal. Chem*., 2014, **86**, 4423-4430.

5 X. Zhu, X. Zuo, R. Hu, X. Xiao, Y. Liang and J. Nan, *Mater. Chem. Phys*., 2014, **147**, 963-967.

6 J. Lou, S. Liu, W. Tu and Z. Dai, *Anal. Chem.*, 2015, **87**, 1145-1151.

7 W. Xu, Y. Xiong, W. Lai, Y. Xu, C. Li and M. Xie, *Biosens. Bioelectron*., 2014, **56**, 144-150.

8 T. Li, J. Byun, B. B. Kim, Y. Shin and M. Kim, *Biosen. Bioelectron*., 2013, **42**, 403-408.

9 F. S. Sabet, M. Hosseini, H. Khabbaz, M. Dadmehr and M. R. Ganjali, *Food Chem*., 2017, **220**, 527-532.

10 C. Wang, W. Zhang, J. Qian, L. Wang, Y. Ren, Y. Wang, M. Xu and X. Huang, *Anal. Method*s, 2021, **13**, 462-468.

11 J. Qian, H. Cui, X. Lu, C. Wang, K. An, N. Hao and K. Wang, *Chem. Eng. J*., 2020, **401**, 126017-126025.